



ELSEVIER

Journal of Non-Crystalline Solids 205-207 (1996) 841-845

JOURNAL OF
NON-CRYSTALLINE SOLIDS

Calculation of electronic properties of amorphous alloys

J.C. Swihart^{a,*}, D.M.C. Nicholson^b, G.M. Stocks^b, Y. Wang^b, W.A. Shelton^b,
H. Yang^a

^a Physics Department, Indiana University, Swain Hall West 117, Bloomington, IN 47405, USA

^b Oak Ridge National Laboratory, MS 6114 Bldg 4500S, Oak Ridge, TN 37831, USA

Abstract

The application of the locally-self-consistent-multiple-scattering (LSMS) method to amorphous alloys is described. The LSMS algorithm is optimized for the Intel XP/S-150, a multiple-instruction-multiple-data parallel computer with 1024 nodes and 2 compute processors per node. The electron density at each site is determined by solving the multiple scattering equation for atoms within a specified distance of the atom under consideration. Because this method is carried out in real space, it is ideal for treating amorphous alloys. The code was adapted to the calculation of the electronic properties of amorphous alloys. In these calculations, the potentials in the atomic sphere approximation were determined self-consistently at each site, unlike previous calculations where the potentials were determined self-consistently at an average site. With these self-consistent potentials, the electronic properties of various amorphous alloy systems were then calculated. The calculated total electronic densities of states are presented for amorphous $\text{Ni}_{80}\text{P}_{20}$ and $\text{Ni}_{40}\text{Pd}_{40}\text{P}_{20}$ with 300 atoms in a supercell.

1. Introduction

In the past [1], we have carried out calculations of the electronic properties of various concentrations of NiP amorphous alloys in the local density approximation (LDA) in which the atoms were arranged in a supercell and relaxed using Weber-Stillinger potentials. The electronic wave functions were determined by a linearized Korringa-Kohn-Rostocker (KKR) band-structure calculation within the LDA. Spherical muffin-tin potentials were used which, for a particular concentration, were determined self-consistently from a separate KKR coherent-potential-approxima-

tion (CPA) calculation on a random alloy in which the atoms were placed at random on an fcc lattice. Thus, the potentials were not determined self-consistently for the particular arrangement of the atoms in the supercell for the amorphous alloy.

The results of these calculations produced densities of states and electrical resistivities due to disorder scattering in quite good agreement with experimental results, although the variation of the resistivities with concentration appeared to be somewhat less than experiment. We also calculated the thermopower, and we found a variation with concentration which was in reasonable agreement with experiment. However, we did not find a change in sign of the thermopower with concentration that was found experimentally.

LSMS is a real-space, multiple-scattering method

* Corresponding author. Tel.: +1-802 855 1247; fax: +1-812 855 5533.

for solving the Kohn–Sham equations that is well-suited for massively parallel computers. We have made the relatively minor changes in the code needed to apply this method to supercell models of amorphous alloys. The advantages of using this method over our earlier procedures are several. First, with LSMS we can now determine the potential self-consistently at each site in the supercell. Second, we can go to a larger number of atoms in the supercell. In our previous serial calculations on a Cray YMP, we were limited to about 340 atoms in the cell. With our LSMS calculations on the Intel Paragon XP/S-150 on which we assign one atom to a node, we can have as many as 1024 atoms in the cell. Finally, with our previous serial calculations on the YMP with 340 atoms, because of memory limitations, we had to confine our angular momentum decomposition sums to an $l_{\max} = 2$. With LSMS on the XPS150 we can handle up to $l_{\max} = 3$ or 4.

In the next section, we discuss briefly the LSMS method. In Section 3, we discuss our calculational procedures. In Section 4, we present our results for the calculated density of states of amorphous NiP and amorphous NiPdP alloys. In Section 5, we discuss our results, and in Section 6 we give our conclusions.

2. Locally-self-consistent-multiple-scattering method

The LSMS method [2] is a single-electron, real-space, multiple-scattering approach based on LDA. This method is ideally suited for calculating the electronic properties of a large number N of atoms (N up to the number of nodes which is currently 1024 on the XP/S-150) in a supercell by massively parallel supercomputers because it exhibits linear ($O(N)$) scaling. At the heart of the LSMS method is the observation that a good approximation to the electron density $\rho^i(r)$ on atom site i can be obtained by considering only the electronic multiple-scattering processes in a limited spatial region about the site i . The cluster of M atoms inside this region is referred to as the local interaction zone (LIZ) for atom i . Each atom is at the center of its own unique LIZ. In solving the Schrödinger equation to obtain $\rho^i(r)$ based at site i , one replaces the effect of all of the

atoms outside the LIZ of atom i by a constant potential. The potential that is to be used in the next self-consistent field (SCF) iteration is calculated by solving Poisson's equation for an electron density made up of all of the single-site densities ρ^i . A real-space multiple scattering approach is also being used by Arnold and Solberg [3].

In our calculations, we assigned each atom in the supercell to its own node on the Intel Paragon XPS150 parallel computer at Oak Ridge National Laboratory. Starting with an initial assumed potential we calculate the scattering path matrix $\tau_{jk}^i(\epsilon)$ at site i with $j, k = 1, 2, \dots, M$. The scattering path matrix is the inverse of the real space KKR matrix $\mathbf{t}^{-1}(\epsilon) - \mathbf{g}(\epsilon)$ where \mathbf{t} is the single-site t -matrix, \mathbf{g} is the real space structure constant matrix, and ϵ is the electron energy. With a maximum angular momentum of $l_{\max} = 3$, the KKR matrix that must be inverted on each node is of dimension 16 times M . The Green's function, and from this the charge density at site i , can be determined from the scattering path matrix. With this we then obtain a new potential for the next iteration. These iterations are carried to convergence at which point we have a self-consistent electron potential at each site.

3. Calculational procedures

For our preliminary calculations using LSMS to determine electronic properties of amorphous alloys, we have examined amorphous $\text{Ni}_{80}\text{P}_{20}$ and $\text{Ni}_{40}\text{Pd}_{40}\text{P}_{20}$. These are interesting systems to compare because, although both can be produced as amorphous systems, the NiPdP system can be made in the amorphous form with slow cooling from the melt [4] whereas NiP alloys become amorphous only with very rapid cooling from melt. The NiPdP alloys can thus be produced as amorphous materials in bulk three-dimensional samples. Such alloy systems could have important potential applications. Thus, it is of interest to determine on a microscopic scale the differences between these two systems.

We have used the atomic sphere approximation (ASA) with overlapping spheres to represent our potential. The ASA sphere volume at a site is taken to be equal to that of the Voronii polyhedron surrounding it. Thus, each site has a different ASA sphere radius.

We report here on results for the electronic density of states determined using one sample of 300 atoms for the supercell for each of the two alloys. The sample was constructed by relaxing with pair potentials a dense random packing of hard spheres as described in Ref. [1]. The sample was shown to agree with experimental partial pair distribution functions of $\text{Ni}_{80}\text{P}_{20}$. Unfortunately partial pair distribution functions are not available for $\text{Ni}_{40}\text{Pd}_{40}\text{P}_{20}$. Furthermore, the density has not been published. We therefore took the sample for $\text{Ni}_{40}\text{Pd}_{40}\text{P}_{20}$ to be identical to that for $\text{Ni}_{80}\text{P}_{20}$ except that half the Ni atoms were replaced at random with Pd.

The LIZ was taken to have a radius of 5.1 AU which includes the nearest neighbor shell of atoms. Other calculations indicate that this size LIZ is sufficient to give electron densities and potentials such that evaluation of the LDA energy using these electron densities and potentials and evaluating the eigenvalue sum using a large LIZ radius (approximately 10.0 AU) will give total energies accurate to tenths or hundredths of a mRy. The fact that the energy can be accurately determined using electron densities calculated with a small LIZ radius is related to the stationarity of the energy with respect to the

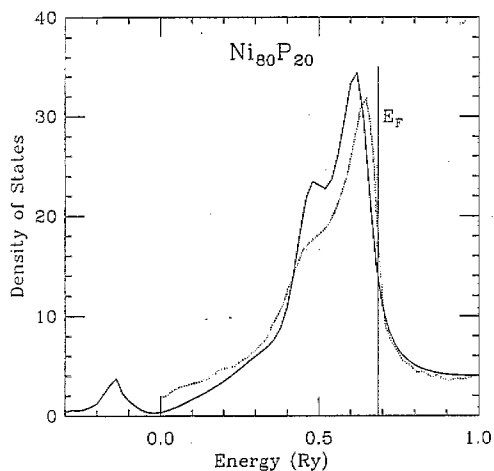


Fig. 1. Calculated electronic density of states (in $\text{Ry}^{-1} \text{atom}^{-1}$ for both spins) for amorphous $\text{Ni}_{80}\text{P}_{20}$. The solid line is for our present calculation with 300 atoms in a supercell and using LSMS converged to self-consistent potentials at each site. The dotted curve is from a previous calculation [2] and represents an average over several supercells with 160 atoms in each cell. For the dotted curve, the potentials were self consistent only for an average site.

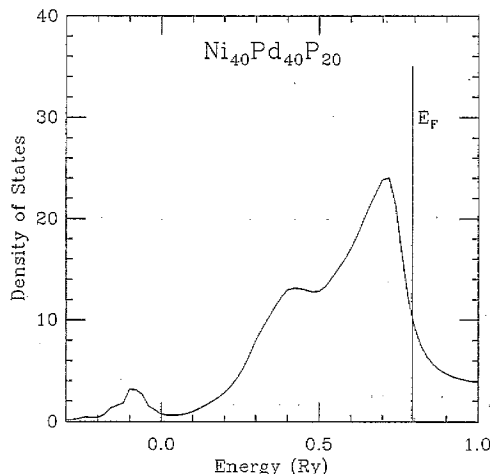


Fig. 2. Calculated electronic density of states (in $\text{Ry}^{-1} \text{atom}^{-1}$ for both spins) for amorphous $\text{Ni}_{40}\text{Pd}_{40}\text{P}_{20}$ with 300 atoms in a supercell. For the calculation we used LSMS converged to self-consistent potentials at each site.

electron density. Unfortunately there is no stationarity principle to insure the accuracy of the density of states. We anticipate that the density of states shown here will be very close to densities of states calculated with a LIZ radius taken to convergence.

4. Results for NiP and NiPdP amorphous alloys

After iterating the calculations for the self-consistent potential to convergence for the $\text{Ni}_{80}\text{P}_{20}$ sample of 300 atoms, we can examine the charge transfer at each Ni and at each P site. In terms of the number of electrons transferred to a particular site (a positive number means that electrons, or negative charge, has been transferred to that site while a negative number means just the opposite), we find that the maximum transfer to the 240 Ni sites is 0.574, the minimum is -0.096 , and the average transfer is 0.169. For the 60 P sites, the maximum is -0.269 , the minimum is -0.997 and the average is -0.675 .

For both the $\text{Ni}_{80}\text{P}_{20}$ and the $\text{Ni}_{40}\text{Pd}_{40}\text{P}_{20}$ samples, we calculated the total electronic density of states for the converged potentials. Fig. 1 shows the calculated density of states for $\text{Ni}_{80}\text{P}_{20}$. The solid curve is the result of the present calculation in which the potential is determined self-consistently at each

site, while the dotted curve is for a previous calculation [1] in which the potential was not determined self-consistently.

Fig. 2 gives the result of our calculation of the electronic density of states for our 300 atom sample of $\text{Ni}_{40}\text{Pd}_{40}\text{P}_{20}$ with the potential determined self-consistently at each site.

5. Discussion

The amount of charge transferred at each atomic site compared to the neutral atom depends very much on the particular volume taken around the atom. Thus, the actual value for the charge transfer has limited significance. However, a comparison of the charge transfer values among all the Ni atoms or among all the P atoms gives an indication of the variation of local environments among all of the atoms of a given species in the sample. The point is that the large variation that we find for our samples of amorphous $\text{Ni}_{80}\text{P}_{20}$ and $\text{Ni}_{40}\text{Pd}_{40}\text{P}_{20}$ after the potentials have been determined self-consistently indicate that there are large variations in the potentials among the atoms of a given species in the sample.

On comparing the electronic density of states of $\text{Ni}_{80}\text{P}_{20}$ calculated here with self-consistent potentials (Fig. 1, solid line) and an earlier calculation [1] in which there was one Ni potential used for all the Ni sites and one P potential used for all the P sites (Fig. 1, dotted line), we note several points of qualitative agreement. Both calculations exhibit a large d-band peak of roughly the same width, and the position of the peak is at about the same energy with respect to the Fermi level. Also the density of states at the Fermi level is approximately the same in the two cases. This last value has important consequences in determining the specific heat and the transport properties. Our earlier calculation produced quite good agreement with experiment for these properties. Serious calculation of the specific heat and transport properties would entail greatly extending the LIZ. It is likely that such an extension of the LIZ would broaden the density of states and move the Fermi level up slightly. Therefore at this point, we are not concerned about the difference between the LSMS density of states at E_F and our earlier work.

There are also quantitative differences between the two calculations. The d-band density of states is broader, and its peak occurs closer to the Fermi level for the earlier calculation compared to the present one. The density of states at the Fermi level is about 15% lower in the present calculation than in the earlier one. Also the present calculation produced a second smaller peak at about 0.2 Ry below the Fermi level while the earlier calculation has only a shoulder in this energy region.

The calculated electronic density of states that we found for $\text{Ni}_{40}\text{Pd}_{40}\text{P}_{20}$, Fig. 2, differs considerably from that of $\text{Ni}_{80}\text{P}_{20}$, Fig. 1. As one would expect, because Pd is a much larger atom than Ni, the overlap between Pd d-orbitals and the d-orbitals on neighboring Ni and Pd atoms results in a density of states with a much wider d-band peak as shown in Fig. 2. Recall that we have fixed the atomic positions at the values appropriate for $\text{Ni}_{80}\text{P}_{20}$, with no scaling to larger volume to accommodate the larger Pd atoms. However the pressure calculated at this volume is only slightly positive indicating that the equilibrium volume is not much larger for $\text{Ni}_{40}\text{Pd}_{40}\text{P}_{20}$ than for $\text{Ni}_{80}\text{P}_{20}$. Relaxations other than simple scaling will tend to increase the Pd–Pd and Pd–Ni bond lengths and narrow the density of states. The density of states at the Fermi level is approximately 25% smaller for the $\text{Ni}_{40}\text{Pd}_{40}\text{P}_{20}$ compared to the $\text{Ni}_{80}\text{P}_{20}$.

6. Conclusions

We have demonstrated that we can apply the LSMS method to amorphous alloys represented by a supercell of 300 atoms and can determine the potential at each atomic site self-consistently on a massively parallel supercomputer. We have found that the charge transfer varies appreciably from site to site for the same species in a given sample indicating that the use of potentials made self-consistent only at an average site is of limited validity. We have also demonstrated that we can use the fully self-consistent potentials to calculate electronic properties of these alloys. We have found the electronic density of states for one sample with 300 atoms representing amorphous $\text{Ni}_{80}\text{P}_{20}$ and one sample with 300 atoms representing amorphous $\text{Ni}_{40}\text{Pd}_{40}\text{P}_{20}$.

For future work, we plan to go to larger samples and to explore more fully the dependence of our results on both sample size and the size of the local interaction zone. We also plan to extend the calculations to determining transport properties and the free energy.

Acknowledgements

This work was supported in part by the ORNL Partnership in Computational Sciences (PICS) Program, supported by the Department of Energy's Mathematical Information, and Computational Science (MICS) Division of the Office of Computational Technology Research. Additional support was provided by the Division of Materials Science, Of-

fice of Energy Research, US DOE under contract No. DEAC05-84OR21400 with Lockheed Martin Energy Systems.

References

- [1] H. Yang, J.C. Swihart, D.M. Nicholson and R.H. Brown, *Phys. Rev. B* 47 (1993) 107; *Mater. Res. Soc. Symp. Proc.* 291 (1993) 419.
- [2] D.M.C. Nicholson, G.M. Stocks, Y. Wang, W.A. Shelton, Z. Szotek and W.M. Temmermann, *Phys. Rev. B* 50 (1994) 14686; Y. Wang, G.M. Stocks, W.A. Shelton, D.M.C. Nicholson, Z. Szotek and W.M. Temmermann, *Phys. Rev. Lett.* 75 (1995) 2867.
- [3] R. Arnold and H. Solbrig, *J. Non-Cryst. Solids* 189 (1995) 129; these Proceedings, p. 861.
- [4] A.J. Drehman and A.L. Greer, *Acta Metall.* 32 (1984) 323.